

This document is confidential and is proprietary to the American Chemical Society and its authors. Do not copy or disclose without written permission. If you have received this item in error, notify the sender and delete all copies.

Exciton Delocalization in Indolenine Squaraine Aggregates Templated by DNA Holliday Junction Scaffolds

Journal:	<i>The Journal of Physical Chemistry</i>
Manuscript ID	jp-2020-06480y.R2
Manuscript Type:	Article
Date Submitted by the Author:	01-Oct-2020
Complete List of Authors:	Mass, Olga; Boise State University, Micron School of Materials Science and Engineering Wilson, Christopher; Boise State University, Micron School of Materials Science and Engineering Roy, Simon; Boise State University College of Engineering, Micron School of Materials Science and Engineering Barclay, Matthew; Boise State University Micron School of Materials Science and Engineering Patten, Lance; Boise State University, Micron School of Materials Science and Engineering Terpentschnig, Ewald; SETA BioMedicals Lee, Jeunghoon; Boise State University, Chemistry and Biochemistry; Boise State University, Micron School of Materials Science and Engineering Pensack, Ryan; Boise State University, Micron School of Materials Science & Engineering Yurke, Bernard; Boise State University, Micron School of Materials Science & Engineering/Department of Electrical & Computer Engineering Knowlton, William; Boise State University, Micron School of Materials Science & Engineering; Department of Electrical and Computer Engineering

SCHOLARONE™
Manuscripts

1
2
3
4
5
6
7
8
9
10
11
12
13
14
15
16
17
18
19
20
21
22
23
24
25
26
27
28
29
30
31
32
33
34
35
36
37
38
39
40
41
42
43
44
45
46
47
48
49
50
51
52
53
54
55
56
57
58
59
50

Exciton Delocalization in Indolenine Squaraine Aggregates Tempered by DNA Holliday Junction Scaffolds

¹*Olga A. Mass; ¹Christopher K. Wilson; ¹Simon K. Roy; Matthew S. Barclay; ¹Lance K. Patten;
²*Ewald A. Terpetschnig; ^{*1,3}Jeunghoon Lee; ^{*1}Ryan D. Pensack; ^{*1,4}Bernard Yurke; ^{*1,4}William
B. Knowlton.**

¹Micron School of Materials Science & Engineering, ³Department of Chemistry and
Biochemistry, ⁴Department of Electrical & Computer Engineering, Boise State University,
Boise, Idaho 83725, United States

²SETA BioMedicals, LLC, 2014 Silver Court East, Urbana, IL 61801, United States

1
2
3
4
5
6
7
8
9
10
11
12
13
14
15
16
17
18
19
20
21
22
23
24
25
26
27
28
29
30
31
32
33
34
35
36
37
38
39
40
41
42
43
44
45
46
47
48
49
50
51
52
53
54
55
56
57
58
59
50
60
ABSTRACT

Exciton delocalization plays a prominent role in the photophysics of molecular aggregates, ultimately governing their particular function or application. DNA is a compelling scaffold in which to template molecular aggregates and promote exciton delocalization. As individual dye molecules are the basis of exciton delocalization in molecular aggregates, their judicious selection is important. Motivated by their excellent photostability and spectral properties, here we examine the ability of squaraine dyes to undergo exciton delocalization when aggregated via a DNA Holliday junction (HJ) template. A commercially available indolenine squaraine dye was chosen for the study given its strong structural resemblance to Cy5, a commercially available cyanine dye previously shown to undergo exciton delocalization in DNA HJs. Three types of DNA-dye aggregate configurations—transverse dimer, adjacent dimer, and tetramer—were investigated. Signatures of exciton delocalization were observed in all squaraine-DNA aggregates. Specifically, strong blue shift and Davydov splitting were observed in steady-state absorption spectroscopy and exciton-induced features were evident in circular dichroism spectroscopy. Strongly suppressed fluorescence emission provided additional, indirect evidence for exciton delocalization in the DNA-templated squaraine dye aggregates. To quantitatively evaluate and directly compare the excitonic Coulombic coupling responsible for exciton delocalization, the strength of excitonic hopping interactions between the dyes were obtained by simultaneous fitting the experimental steady-state absorption and CD spectra via a Holstein-like Hamiltonian in which, following the theoretical approach of Kühn, Renger, and May, the dominant vibrational mode is explicitly considered. The excitonic hopping strength within indolenine squaraines was found to be comparable to that of the analogous Cy5 DNA-templated

1
2
3 aggregate. The squaraine aggregates adopted primarily an H-type (dyes oriented parallel to each
4 other) spatial arrangement. Extracted geometric details of dye mutual orientation in the
5 aggregates enabled close comparison of aggregate configurations and the elucidation of the
6 influence of dye angular relationship on excitonic hopping interactions in squaraine aggregates.
7
8 These results encourage the application of squaraine-based aggregates in next generation systems
9 driven by molecular excitons.
10
11
12
13
14
15
16
17
18
19
20
21
22
23
24
25
26
27
28
29
30
31
32
33
34
35
36
37
38
39
40
41
42
43
44
45
46
47
48
49
50
51
52
53
54
55
56
57
58
59
60

INTRODUCTION

Exciton delocalization often plays a decisive role in governing the photophysical properties of molecular aggregates, ultimately determining their suitability for particular applications. A well-established framework for understanding exciton delocalization in molecular aggregates, and associated excitonic coupling responsible for delocalization, is the molecular exciton model developed by Kasha.¹ In Kasha's molecular exciton model, exciton delocalization results from the collective excitation of the locally excited states of an array of proximate dye molecules forming a molecular aggregate.

Described in Kasha's molecular exciton model, the excitonic hopping parameter, $J_{m,n}$, is the strength of that component of the Coulombic coupling (electrodynamic interactions²) between dye m and dye n (within a molecular aggregate) that induces a transition from the excited state of one molecule while simultaneously inducing a transition from the ground state to the electronic excited state of the other molecule. Thereby an excitation is transferred from one molecule to the other. This is a hopping interaction and is referred to in the literature in a number of categorical ways in terms of interaction, hopping, and coupling or in the context of a parameter, shift or potential. Relative to the former, $J_{m,n}$ is referred to as an exchange interaction,³⁻⁴ instantaneous intermolecular interaction,⁵ resonant interaction or coupling,⁶⁻⁸ resonant exciton hopping,⁹ intermolecular Coulombic interaction,¹⁰⁻¹⁴ intermolecular dipole-dipole coupling,¹⁵ long-range dipole-dipole Coulombic interaction,¹⁶ excitonic coupling,¹⁷ and electronic interaction.¹⁸⁻¹⁹ In the context of the latter, $J_{m,n}$ is called a hopping parameter,²⁰ monoexcitonic shift,²¹ and point-dipole interaction potential.²² Although not a complete list, the number of ways $J_{m,n}$ is described suggests that a more thorough description may be useful. The excitonic hopping interaction inherent in $J_{m,n}$ enables exciton delocalization and relaxation.^{5, 7-8, 11-13} Where intermolecular

distances are less than ~ 4 Å (e.g., aggregates with π -stacking or covalently bridged), wave function overlap can induce intermolecular charge transfer (also described as superexchange coupling or Dexter mechanism, coupling or interaction) and could contribute to the $J_{m,n}$ term.^{11-13, 16, 18-20} In our work, it is assumed that intermolecular charge transfer can be neglected. It should be noted that $J_{m,n}$ is often approximated as the coupling between a pair of transition point dipoles and is referred to as such. In our analysis, the point dipole approximation was deemed inadequate since the spacing between the dyes is shorter than their length. Instead, an extended dipole approximation²³ was employed where the dipoles are modeled as two point charges of opposite sign separated by nearly the length of the dye core. This extended dipole approximation better accounts for the physical charge distribution that spreads out over the length of the molecule with the maxima of charge density occurring near the ends of the dye.

Exciton delocalization in molecular aggregates was first observed in the 1930s by Jelley and Scheibe, who independently noted large shifts in the absorption spectra of molecular aggregates as compared to that of the respective monomers.²⁴⁻²⁶ Exciton delocalization has also been observed in molecular aggregates present in natural light harvesting systems.²⁷⁻³¹ The rational control of exciton delocalization in molecular aggregates in synthetic, or artificial, systems has significant implications on next generation technologies, such as artificial light harvesting,³² nanoscale excitonic computing,³³⁻³⁷ solar energy conversion,^{32, 38-39} and on fundamental studies of quantum entanglement⁴⁰⁻⁴³ in molecular aggregates, which may benefit potential applications in room temperature quantum information systems.⁴⁴⁻⁴⁵

A rational control of exciton delocalization in molecular aggregates requires the judicious selection of the constituent molecules, or dyes, and control of their spatial arrangement. Exciton delocalization was originally observed in concentrated solutions (i.e., well above the solubility

1
2
3 limit), which promoted the formation of large dye aggregates via their spontaneous precipitation
4 out of solution.^{24-26, 46-48} The ability to rationally control exciton delocalization via the number of
5 dyes and their spatial arrangement in dye aggregates formed via spontaneous precipitation,
6 however, has significant limitations. In natural systems, in contrast, a protein matrix is used to
7 organize a precise number of dyes and maintain precise control of their relative distance and
8 orientation.^{44, 49-53} While the assembly of dye aggregates via proteins affords exquisite control
9 over dye aggregation, the intricate design rules of protein folding and dye-protein interactions
10 substantially complicates the rational use of protein nanostructures as scaffolds.⁵⁴⁻⁵⁷ The design
11 rules associated with an alternative biomacromolecule, deoxyribonucleic acid (DNA), are
12 comparatively much simpler. Because there are only four nucleic acid building blocks in DNA
13 that associate via Watson-Crick pairing, design rules to rationally and predictably synthesize
14 complex DNA nanostructures are increasingly mature and compelling.^{58-59, 60-61} Critically, the
15 controlled assembly of dye aggregates in DNA has been demonstrated. Generally, there are two
16 approaches to control the assembly of dye aggregates via DNA, either via noncovalent
17 interaction of dyes with DNA⁶²⁻⁷² or via direct covalent binding of dyes to DNA.⁷³⁻⁸⁵ While
18 templating of dye aggregates via their noncovalent intercalation with DNA offers improved
19 control over the spontaneous assembly,⁶²⁻⁷² the approach still confers limited control over the
20 number of dyes in the aggregate and their spatial arrangement since the aggregation is induced in
21 concentrated solutions and via noncovalent interactions with specific base pairs in the minor
22 groove of long sequences of double-stranded, or duplex, DNA (dsDNA). Direct covalent binding
23 of dyes to DNA, in contrast, provides more extensive control of the number of dyes in the
24 aggregate and their spatial arrangement. Direct covalent binding of dyes to DNA enables: (i)
25 choice of the type of dye,^{75, 77} (ii) choice of the number of dyes,^{22, 83} including assembly into large
26

1
2
3 two- and three-dimensional dye aggregate arrays, and (iii) the precise positioning of the dyes
4 along the DNA backbone,^{66, 74-75, 77-79, 81} which confers control over their spatial arrangement.
5
6
7
8 Numerous studies have demonstrated exciton delocalization in dye aggregates templated within
9
10 dsDNA structures,^{74-82, 85-96} even within more complex, higher-order DNA nanostructures.^{75, 97}
11
12

13 Among the many types of dyes employed in DNA-templated aggregation,^{74-82, 86-93} cyanine
14 dyes, a well-known group of a broader family of polymethine dyes, have established a particular
15 prominence. Of especial note is the commercially available cyanine dye Cy5 (**Fig. 1a**), which is
16 a pentamethine dye that exhibits an intense absorption profile in the visible (specifically, the red)
17 part of the electromagnetic spectrum. Taking advantage of the optimal photophysical properties
18 of Cy5, whose visible electronic absorption exhibits a large peak extinction coefficient of
19 ~250,000 cm⁻¹ M⁻¹ at ca. 650 nm, our group recently demonstrated exciton delocalization in
20 dimers, trimers, and tetramers of Cy5 templated using both dsDNA and a four-armed DNA
21 Holliday Junction (HJ)⁹⁸⁻⁹⁹ scaffolds.¹⁰⁰⁻¹⁰¹ Proximate Cy5 dyes at distances of <1 nm in the core
22 of the DNA HJ resulted in extensive spectral shifts, evident via significant Davydov splitting¹⁰²
23 (i.e., splitting of the monomer peak – one red-shifted and the other blue-shifted), indicative of
24 strong exciton coupling and exciton delocalization. A benefit of employing a DNA HJ as a
25 scaffold over lower-order DNA, such as dsDNA, is that it enables the assembly of up to 4 dyes in
26 the core of HJ. As a result, different dimer, trimer, and tetramer dye aggregate configurations can
27 be selectively accessed by templating via a DNA HJ. At the same time, aggregation beyond the
28 desired number of dyes is suppressed. Additionally, Cannon *et al.* showed that the packing
29 behavior of the Cy5 dyes could be controlled, i.e., either J- or H-type aggregate packing
30 arrangements could be promoted, when two dyes were positioned on adjacent or opposite arms
31 of the DNA HJ, respectively.¹⁰¹ Despite their remarkable spectral properties, concerns remain
32
33
34
35
36
37
38
39
40
41
42
43
44
45
46
47
48
49
50
51
52
53
54
55
56
57
58
59
60

regarding the general utility of Cy5 aggregates given the dye's strong susceptibility to photooxidation and photoisomerization.¹⁰³⁻¹⁰⁴

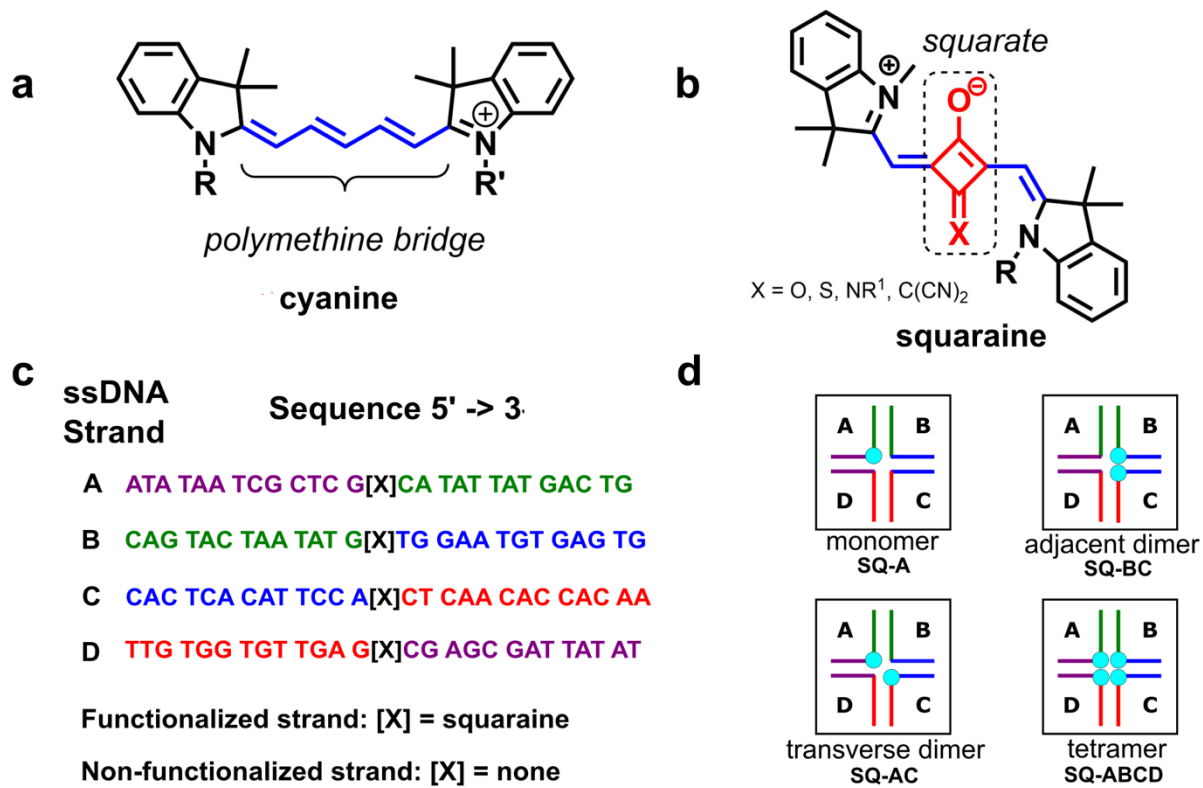


Figure 1. (a) A representative example of the chemical structure of cyanine dye Cy5 where R, R' – sites of attachment to DNA through phosphoramidite linkers. (b) A representative example of the chemical structure of core-substituted indolenine squaraine dye, where X= O, S, NR¹, C(CN)₂; R – a site of attachment to DNA through a serinol linker and R¹ is an alkyl (also see **Fig. S1**). (c) asymmetrical DNA sequences to assemble immobile Holliday junctions; complementary regions of ssDNA are color-coded: *e. g.* a purple region of strand A is complementary to a purple region of strand D, and a green region of strand A is complementary to a green region of strand B *etc.* (d) Schematic representation of dye monomer, dimers, and a tetramer in four-armed

1
2
3 duplex DNA junctions (Holliday junction) where squaraine dyes are depicted as blue dots. As
4
5 discussed in **Sections S3 and S10**, the DNA HJ may exist primarily in a stacked conformation.
6
7 ssDNA strands used to assemble DNA HJ are labeled as A, B, C, and D.
8
9

10
11 Squaraines (also known as squarylium dyes) are a family of dyes that exhibit improved
12 photochemical stability in addition to optical properties similar to cyanines.¹⁰⁵⁻¹⁰⁸ Similar to
13 cyanines, squaraines are characterized by an intense absorption profile in the visible and near-
14 infrared regions of the electromagnetic spectrum, with peak extinction coefficients in the range
15 of ~200,000 - 250,000 M⁻¹ cm⁻¹. While their optical properties are similar, squaraines structurally
16 differ from cyanines due to the incorporation of a squarate moiety in the center of the
17 polymethine bridge (**Fig. 1b**). Though squaraines can contain various aromatic (*e.g.* aniline,
18 phenol, azulene) and heterocyclic (*e.g.* pyrroline, indolenine, benzothiazole) rings, all derivatives
19 of squaraines have in common the central squarate moiety. The central squarate moiety confers
20 improved photochemical stability by inhibiting oxidation of the polymethine bridge and limiting
21 the ability of the polymethine bridge to undergo photoinduced rotational motion, or
22 isomerization. Originally developed in 1965 by Treibs and Jacob,¹⁰⁹ squaraines and squaraine
23 aggregates have since been utilized in a variety of applications ranging from photovoltaic
24 devices¹¹⁰⁻¹¹² to sensors¹¹³ and fluorescent labels in biomedicine.^{111-112, 114} Aggregation of squaraine
25 dyes has been observed in concentrated solution¹¹⁵⁻¹¹⁶ and upon conjugation to protein.¹⁰⁸ The
26 excitonic coupling was studied experimentally and theoretically in the covalently linked bis-
27 squaraine dimers exhibiting J-type behavior.¹¹⁷⁻¹¹⁸ However, to our knowledge, there is only one
28 report describing DNA-induced aggregation of squaraines studied on the one form of an
29 indolenine-type (*i.e.* squaraines containing indolenine rings on both sides of the squaraine moiety)
30 squaraine dimer attached to a short DNA duplex.⁷⁶ The reported squaraine dimer was observed to
31
32
33
34
35
36
37
38
39
40
41
42
43
44
45
46
47
48
49
50
51
52
53
54
55
56
57
58
59
60

1
2
3 exhibit an H-type packing with spectral signatures of strong exciton interactions, however, the
4 exciton interactions were not evaluated quantitatively.
5
6

7
8 In this study, we examine exciton delocalization in a broader range of squaraine aggregates (i.
9 e., -mers): two dimer aggregates and a tetramer, templated by a DNA HJ. Given the structural
10 similarity of cyanines and squaraines—and given the excellent results observed with aggregates
11 of Cy5 templated in DNA HJ¹⁰⁰⁻¹⁰¹—we hypothesized that similar excitonic Coulombic coupling
12 and delocalization could be achieved in DNA HJs of squaraine dyes. To facilitate the comparison
13 with Cy5 containing indolenine rings at both ends of the pentamethine bridge (**Fig. 1a**), we
14 chose a commercially available squaraine dye featuring indolenine rings on both sides of the
15 squarate moiety (**Fig. 1b**), which we subsequently refer to as indolenine squaraine. As
16 representative dye aggregates (i.e., -mers), we assembled a transverse dimer, an adjacent dimer
17 and a tetramer in the core of an immobile DNA HJ containing asymmetrical sequences (**Fig. 1c**)
18 to prevent branch migration. Signatures of the exciton delocalization were observed in the
19 steady-state absorption and circular dichroism (CD) spectra of the DNA-templated squaraine dye
20 aggregates. The steady-state absorption spectra of the DNA-templated squaraine aggregates
21 exhibited a significant blue shift (i.e., peak shift and redistribution of oscillator strength toward
22 short wavelengths or higher energies) compared with that of the monomer, which is a signature
23 of exciton delocalization and indicates an H-type aggregate packing arrangement that is adopted
24 in all DNA-templated squaraine dye aggregates. The presence of pronounced exciton-coupled
25 CD signals in the circular dichroism spectra represent an additional signature of exciton
26 delocalization. Significant fluorescence quenching observed via steady-state fluorescence
27 emission spectroscopy provided supporting indirect evidence of exciton delocalization. The
28 absorption and CD spectra were modeled theoretically to quantitatively evaluate the excitonic
29 interactions.
30
31
32
33
34
35
36
37
38
39
40
41
42
43
44
45
46
47
48
49
50
51
52
53
54
55
56
57
58
59
60

1
2
3 hopping parameter $J_{m,n}$, that characterizes the strengths of excitonic Coulombic couplings
4 responsible for exciton delocalization in the DNA-templated squaraine aggregates. The modeling
5 derived appreciable $J_{m,n}$ values, comparable in magnitude to $J_{m,n}$ values responsible for exciton
6 delocalization in the analogous DNA-templated Cy5 aggregate. The details of spatial
7 arrangement of the constituent squaraines in H-aggerates were extracted from the modeling
8 providing insights on how the geometry parameters affect excitonic Coulombic couplings
9 strength.
10
11
12
13
14
15
16
17
18
19
20
21
22
23
24
25
26
27
28
29
30
31
32
33
34
35
36
37
38
39
40
41
42
43
44
45
46
47
48
49
50
51
52
53
54
55
56
57
58
59
60

METHODS

Sample preparation.

DNA oligomers internally functionalized with Square 660-NHS (K8-1352, SETA BioMedicals, Urbana-Champaign, IL) via a non-nucleosidic amino serinol sequence modifier and purified via dual high-performance liquid chromatography were purchased from Bio-Synthesis, Inc. Non-functionalized DNA oligomers purified by standard desalting were purchased from Bio-Synthesis, Inc. All DNA oligomers were rehydrated in ultrapure water (Barnstead Nanopure, Thermo Scientific) to prepare 100 μ M stock solutions. Concentrations of DNA samples were determined spectroscopically on NanoDrop One Microvolume UV-Vis (Thermo Scientific) using calculated extinction coefficients. DNA Holliday junctions were prepared by combining equimolar amounts of complimentary oligomers in 1X TBE, 15 mM MgCl₂ buffer solution to a final DNA concentration 1.5 μ M. All DNA samples were annealed in Mastercycler Nexus PCR cycler (Eppendorf) according to the following protocol: 4 min at 94 °C, followed by cooling ramps: 0.1 °C per 15 sec from 94 °C to 64 °C, and 10 °C per 1 min from 64

1
2
3 °C to room temperature. For the fluorescence measurements, the DNA samples were further
4
5 diluted to 0.5 μ M DNA concentration.
6
7

8 *Optical characterization.*
9

10 UV-Vis spectra were recorded in triplicates at room temperature on dual-beam Cary 5000
11 UV-Vis-NIR spectrophotometer (Agilent Technologies) in a quartz cuvette with 1 cm path
12 length (Starna). Absorbance spectra were monitored over a 230-800 nm wavelength range.
13 Circular dichroism (CD) measurements were performed on a JACSO-J810 spectropolarimeter.
14 DNA samples (120 μ L) were transferred into a 1 cm path length quartz cuvette (Jasco). Spectra
15 were recorded over a 230-800 nm wavelength range (three scans per sample were averaged) at a
16 speed of 200 nm min^{-1} . Steady-state fluorescence spectra were obtained using a Horiba PTI
17 QuantaMaster 400 spectrofluorometer (Horiba Scientific) in a 1 cm path length quartz cuvette
18 (Starna) and monitored as a function of wavelength when excited at $\lambda_{\text{exc}} = 650$ nm. The
19 fluorescence spectra were corrected for the wavelength dependence of the detection system
20 response using the correction curve provided by the manufacturer. The fluorescence spectra were
21 scaled by the absorptance at the excitation wavelength.
22
23
24
25
26
27
28
29
30
31
32
33
34
35
36
37
38
39
40
41
42

43 RESULTS AND DISCUSSION

44 Construct Design and Synthesis

45 Three types of squaraine aggregate constructs, an adjacent dimer, a transverse dimer and a
46 tetramer, were prepared by templating the dyes in the branch point of an immobile DNA HJ. The
47 immobile DNA HJ with arm branch length of 13 base pairs was formed by four asymmetrical
48 single DNA strands A, B, C, and D (26 bases each) (**Fig. 1c**). Because of its large peak molar
49
50
51
52
53
54
55
56
57
58
59
60

extinction and narrow absorption bands, Square 660 was chosen as a representative commercially available indolenine squaraine dye (**Fig. 1b**). To functionalize each DNA strand with the squaraine dye, the dyes were covalently attached through a non-nucleosidic serinol-based linker (**Fig. S1**). Functionalized and non-functionalized strands were used to assemble constructs depicted in **Fig. 1d**. A single Square 660 dye was templated in a DNA HJ to prepare a monomer construct as a control. We denote this configuration as **SQ-A** (**Fig. 1d**). Aggregation of two Square 660 dyes into a dimer was performed using two different configurations. In the transverse configuration **SQ-AC**, two Square 660 dyes were attached to opposing DNA arms A and C; while in the adjacent configuration **SQ-BC**, the two dyes were attached to adjacent DNA arms B and C. Complementary oligo strands were combined in equimolar amounts followed by annealing to ensure complete hybridization. The Square 660 dye aggregates were analyzed by non-denaturing polyacrylamide gel electrophoresis for the presence of remaining single functionalized strands. The amount of unreacted functionalized single strands (i.e., A, B, C, and D) in the aggregate samples did not exceed 5% as estimated by densitometry analysis (**Fig. S2**).

Thermal denaturation experiments were performed to examine the conformation and stability of the DNA HJ templating the squaraine aggregates (**Section S3**). The DNA denaturation was monitored by the absorption in the nucleobase region (260 nm). Resulting sigmoidal curves indicated the cooperative melting of the stacked DNA HJ conformation templating all the squaraine aggregates in the presence of $MgCl_2$ (**Fig. S3**). The formation of stacked DNA HJ conformation was further supported with the comparative melting experiments in the presence of $NaCl$ promoting open DNA HJ conformation (**Fig. S4**). A reference unmodified DNA HJ melted at 60.0 °C in 1X TBE 15 mM $MgCl_2$. The insertion of a single squaraine dye in the DNA HJ through a serinol linker resulted in a slight decrease in the melting point of the **SQ-A** monomer (-

1
2
3 1.7 °C) compared to the unmodified DNA HJ which is equivalent to the dissociation of one
4 canonical AT pair. This result suggests that electronic interactions between a squaraine dye and
5 surrounding nucleobases are repulsive in nature and rather small. The squaraine dimers melted at
6 approximately the same temperature as the unmodified DNA HJ indicating that dye-dye
7 interactions compensate for the insertion of two serinol linkers (**Tbl. S2**). The presence of the
8 four dyes in the **SQ-ABCD** tetramer increased the melting point to 4.5 deg °C compared to the
9 unmodified DNA HJ suggesting strong attractive interaction between the four squaraine
10 molecules with overall stabilizing effect on the dye-DNA construct.
11
12
13
14
15
16
17
18
19
20
21
22
23

24 Steady-State Optical Characterization 25

26 As an individual dye molecule forms the basis of a molecular aggregate, a DNA HJ containing
27 a single Square 660 dye was first prepared and characterized. As our dye monomer reference, we
28 studied Square 660 attached to the A strand and hybridized with all other unlabeled (B-D)
29 strands. The electronic absorption spectrum of **SQ-A** exhibited two prominent absorption
30 spectral bands with peak maxima at 672 and 630 nm (**Fig. 2a**) respectively assigned to the 0-0
31 and 0-1 vibronic transitions of the individual Square 660 dye. The 0-0 band exhibits a peak
32 molar extinction of ca. 192,000 M⁻¹ cm⁻¹, indicative of a strongly allowed electronic transition.
33 Both the minimal vibronic structure and large extinction coefficient (which suggests a large
34 transition dipole moment) are conducive to exciton delocalization and strong excitonic
35 Coulombic coupling, suggesting Square 660 is an excellent candidate for DNA-templated dye
36 aggregates. Strong fluorescence of monomer **SQ-A** was observed with a 0-0 band peaking at 687
37 nm (**Fig. S5**). The difference in energy between the 0-0 band in absorption and the 0-0 band in
38 fluorescence, i.e., the Stokes shift, is 325 cm⁻¹ (40 meV). This value is on the smaller end than
39
40
41
42
43
44
45
46
47
48
49
50
51
52
53
54
55
56
57
58
59
60

1
2
3 that of Cy5 dye monomers attached to DNA (300-600 cm⁻¹ [37-77 meV]),^{100-101, 119} indicating a
4 smaller change in geometry between the ground state and the excited state in the indolenine
5 squaraine, which might result from the more rigid structure of squaraine compared to Cy5 dye.
6
7 The optical characteristics of **SQ-A** are similar to that of the “free” Square 660 dye not attached
8 to DNA, which in a pH 7.0 phosphate buffer, exhibits an absorption 0-0 band peaking at 658 nm
9 (182,000 M⁻¹ cm⁻¹ extinction) and fluorescence 0-0 band peaking at 676 nm (**Fig. S6a**). The
10 difference in spectral characteristics between the monomer **SQ-A** and the “free” dye in solution
11 may be attributable to solvatochromic effects, such as differences in the buffer conditions or the
12 local DNA environment, or other effects such as electronic interactions with nucleobases.
13
14 However, alternating the functionalized strand in the monomer construct (i.e. a squaraine is
15 attached to strand B, C, or D instead of strand A) did not influence the absorption peak maxima
16 indicating that a squaraine does not exhibit strong electronic interactions with surrounding
17 nucleobases (**Fig. S6b**). The **SQ-A** monomer in DNA HJ exhibited high fluorescence quantum
18 yield (Φ_F) measured to be 0.37 (**Section S5**) which is slightly higher than that of Cy5 in ssDNA
19 reported in the range 0.29-0.33.¹¹⁹ The lower quantum yield in Cy5 may be related to torsion
20 motion around the polymethine bridge. Squaraines are less susceptible to torsional motion due to
21 the squarate moiety incorporated into the polymethine bridge.
22
23
24
25
26
27
28
29
30
31
32
33
34
35
36
37
38
39
40
41
42
43
44
45
46
47
48
49
50
51
52
53
54
55
56
57
58
59
60

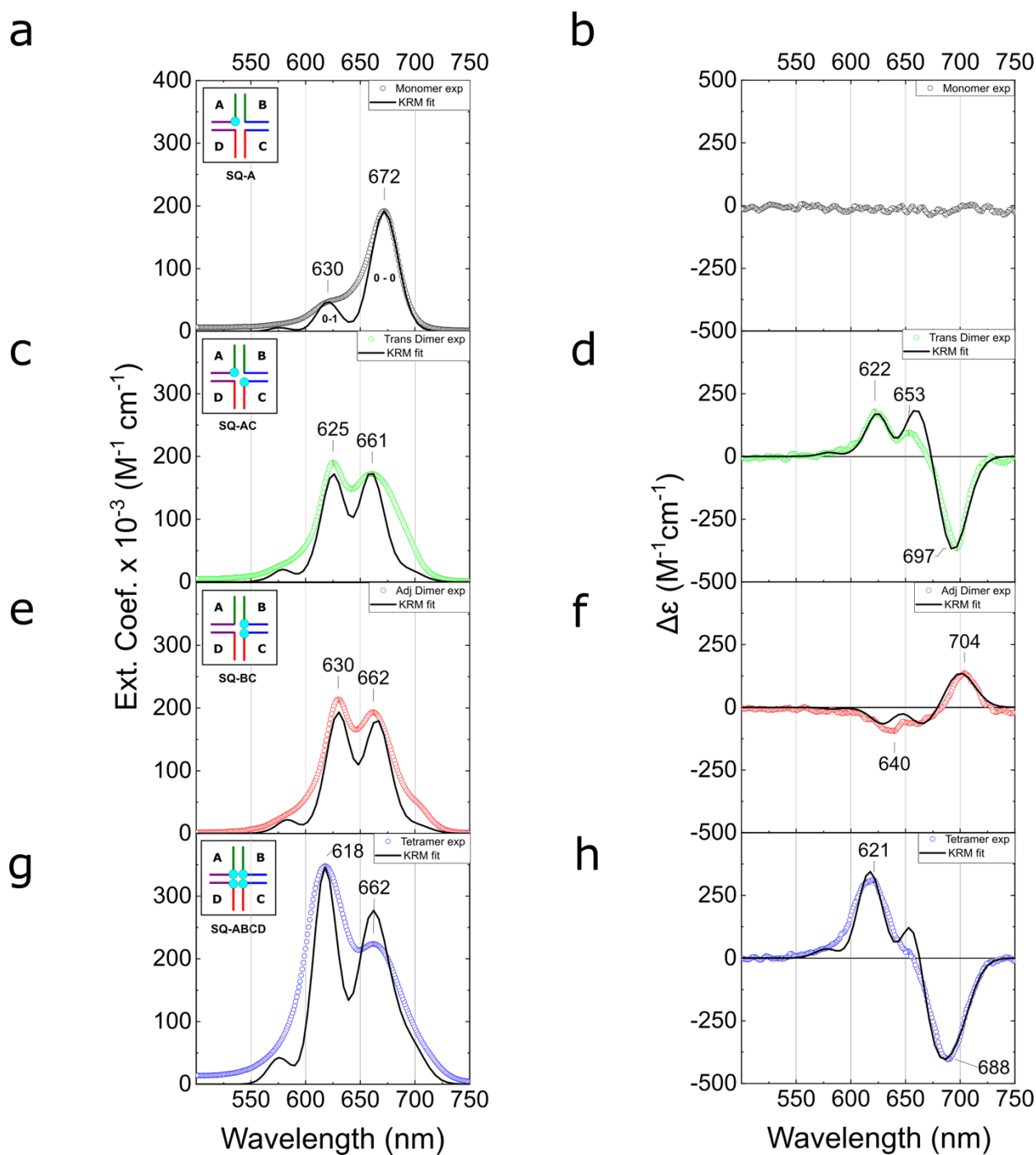


Figure 2. (a, c, e, and g) Acquired steady-state absorption spectra of the DNA-Square 660 dye constructs in 1X TBE, 15 mM MgCl₂ at room temperature (dotted lines) and theoretical absorption spectra derived from KRM modeling (solid lines). The DNA-dye construct concentration was 1.5 μM . The insets show schematic representation of dye monomer, dimers,

1
2
3 and tetramer constructs in DNA HJ. **(b, d, f, h)** Acquired CD spectra of the DNA-Square 660
4 dye constructs in 1X TBE, 15 mM MgCl₂ at room temperature (dotted lines), and theoretical CD
5 spectra derived from KRM modeling (solid lines). The DNA-dye construct concentration was 1.5
6 μM.
7
8
9
10
11
12

13 Guided by the inspiring results of Cannon *et al.* on DNA-templated Cy5 aggregates,¹⁰⁰⁻¹⁰¹ we
14 next investigated aggregates of Square 660 in an immobile DNA HJ in the form of adjacent and
15 transverse dimers. The electronic absorption spectrum of the transverse dimer **SQ-AC** exhibited
16 its most prominent absorption band at 625 nm along with an additional broad feature peaking at
17 661 nm, both blue-shifted with respect to the monomer 0-0 band of 672 nm (**Fig. 2c**). The
18 absorption spectrum of the adjacent dimer **SQ-BC** was overall very similar, characterized by a
19 primary blue-shifted band at 630 nm with another major band at 662 nm (**Fig. 2e**). Such blue
20 shift of the electronic absorption spectrum of the aggregate compared with the monomer is
21 indicative of a dominantly face-to-face, or H-aggregate, orientation of the two Square 660 dyes
22 in both adjacent and transverse configurations. Similar optical behavior was previously observed
23 with the Cy5 transverse dimer templated by an immobile DNA HJ.¹⁰¹ Similar to the squaraine
24 transverse dimer (i.e., **SQ-AC**), the Cy5 transverse dimer formed an H-aggregate with a strong
25 excitonic Coulombic coupling. However, the Cy5 adjacent dimer assembled into a J-type
26 aggregate. Consistent with these observations, Markova *et al.* also observed a propensity of
27 indolenine squaraines for H-aggregate formation. In their studies, two indolenine squaraines,
28 dually-tethered to duplex DNA, formed an H-aggregate,⁷⁶ while two Cy5 dyes formed a J-
29 aggregate in the same duplex configuration.⁷⁴
30
31
32
33
34
35
36
37
38
39
40
41
42
43
44
45
46
47
48
49
50
51
52
53
54
55
56
57
58
59
60

Having identified the aggregate type of the transverse and adjacent Square 660 dimers, we next
proceeded to more incisively evaluate signatures of exciton delocalization in the electronic

absorption spectra. To aid in evaluating signatures of exciton delocalization, the absorption spectra were fit with four Gaussian features. The four-component Gaussian fit was justified mathematically (Section S7), while observations in the CD spectra and theoretical modeling provided additional support for the four-component fit (described in subsequent sections). The four absorption bands associated with the fit, labeled A_1 , A_2 , A_3 and A_4 , exhibit peak maxima for the transverse dimer at 690, 660, 624, and 599 nm, respectively, and for the adjacent dimer exhibit peak maxima at 700, 663, 629, and 603 nm, respectively (Fig. S7ab; Tbl. 1). We attribute the weak, red-shifted absorption band (A_1) to the lowest-energy excitonic state of the H-dimer, with the finite absorption intensity arising from a slight oblique (i.e., non-ideal) orientation of the H-dimer. The Gaussian fitting additionally reveals that while the intensity of the absorption bands of the monomer varies in the order A_1 (0-0) > A_2 (1-0), the intensity of the absorption bands for both dimers varies in the order A_2 > A_1 and A_3 > A_1 . Such redistribution of oscillator strength in the form of a decreased A_n / A_{n+1} ratio¹⁷ (that contributes to the blue shift in the absorption spectrum) is consistent with a large value for the excitonic hopping parameter $J_{1,2}$, and exciton delocalization. Lastly, the magnitude of the energy difference between the low- and high-energy excitonic states, i.e., the so-called Davydov splitting, can provide an estimate of the value of the excitonic hopping parameter, since for dimers its value is approximately one half the Davydov splitting energy. As noted above, the transition to the low-energy excitonic state can be readily assigned to the lowest-energy absorption band (A_1). Assigning the transition to the high-energy excitonic state to a specific absorption band, in contrast, is complicated by the strong vibronic coupling in the squaraine dyes. As such, and to gain qualitative insight into the excitonic Coulombic coupling strengths, we report the Davydov splitting energies (and corresponding excitonic hopping parameters) associated with A_1 and the next two higher-lying

1
2
3 absorption bands (A_2 and A_3) identified via the Gaussian fitting. For the transverse dimer, the A_2 -
4
5 A_1 and A_3 - A_1 Davydov splitting energies are 82 meV (658 cm^{-1}) and 190 meV (1532 cm^{-1}),
6
7 respectively; for the adjacent dimer, the A_2 - A_1 and A_3 - A_1 Davydov splitting energies are 99 meV
8
9 (797 cm^{-1}) and 200 meV (1610 cm^{-1}), respectively. The corresponding excitonic hopping
10
11 parameters estimated from these values for the transverse dimer are 41 meV (329 cm^{-1}) and 95
12
13 meV (766 cm^{-1}), respectively; for the adjacent dimer, they are 49 meV (398 cm^{-1}) and 100 meV
14
15 (806 cm^{-1}), respectively. For comparison, Röhr *et al.* reported very similar coupling strengths (ca.
16
17 800 cm^{-1} or 99 meV) in the J-aggregates of indolenine squaraine dimers created by covalent
18
19 coupling of two squaraine molecules.¹¹⁷ While a quantitative analysis of the excitonic hopping
20
21 parameter in this manner is complicated by the strong vibronic coupling in the squaraine dyes
22
23 and associated ambiguity in assigning the transition to the high-energy exciton state to a
24
25 particular high-energy absorption band, the magnitude of the estimated excitonic hopping
26
27 parameters are clearly large and indicative of exciton delocalization in both dimers.
28
29
30
31
32
33
34
35
36
37
38
39
40
41
42
43
44
45
46
47
48
49
50
51
52
53
54
55
56
57
58
59
60

Table 1. Steady-State Optical Properties of DNA-Templated Square 660 Constructs.

construct	Observed Abs maxima ^a nm	Calculated Abs maxima ^b nm	Observed FL maxima ^c nm	FL Suppression ^d %	Φ_F^e
monomer	630; 672	630; 672	687	n/a	0.37
trans dimer	625; 661	599; 624; 660; 690	688	80	0.038
adj dimer	630; 662	603; 629; 663; 700	690	92	0.023
tetramer	618; 662	578; 618; 663; 694	689	98	0.006

^aMeasurements were carried out in 1X TBE, 15 mM MgCl₂ containing 1.5 μM DNA construct at room temperature. ^bValues for the monomer are obtained from fitting the data with two Gaussians, and the values for the aggregates are obtained from fitting the data with four Gaussians. ^cMeasurements were carried out in 1X TBE, 15 mM MgCl₂ containing 0.5 μM DNA construct at room temperature. Samples were excited at λ_{exc} = 650 nm. ^dFluorescence suppression relative to the monomer was calculated for 665-740 nm range as described in SI. ^eFluorescence quantum yield measured in 1X TBE, 15 mM MgCl₂.

To further elucidate the excitonic delocalization in the squaraine dimers, CD spectroscopy measurements were performed. CD spectra of the monomer, dimer and tetramer constructs showed a positive bisignate signal in the UV region between 230 and 280 nm confirming well-folded B-form DNA duplex of HJ (Fig. S8). The achiral monomer **SQ-A** did not show an induced CD signal in the visible region (Fig. 2b) indicating that the monomer retained conformational freedom in the core of the DNA HJ. The transverse dimer **SQ-AC** exhibited a negative exciton-induced CD couplet (down-up shape from right to left) in the visible part of the

1
2
3 spectrum (**Fig. 2d**) indicating chiral disposition of coupled transition dipole moments. This
4 bisignate character of the exciton-induced CD couplet and its intensity indicates coherent exciton
5 hopping between the dyes.¹²⁰ The cross-point of the CD couplet at ~ 670 nm corresponds to the
6 absorption maximum of the squaraine monomer **SQ-A**. With an intense negative Cotton effect at
7 697 nm ($\Delta\epsilon = -360 \text{ M}^{-1} \text{ cm}^{-1}$), the obliqueness in dye face-to-face orientation is evident from the
8 splitting of positive Cotton effect at 622 nm ($\Delta\epsilon = 175 \text{ M}^{-1} \text{ cm}^{-1}$) and 653 nm ($\Delta\epsilon = 95 \text{ M}^{-1} \text{ cm}^{-1}$).
9 This asymmetry of the CD couplet is also predicted by the theoretical model in one configuration
10 of coupled dipole moments (discussed below). In analogy, the adjacent dimer **SQ-BC** exhibits a
11 CD couplet with positive sign (i.e., up-down shape from right to left) and asymmetric shape (**Fig.**
12 **2f**) but of opposite chirality compared to the transverse dimer **SQ-AC**. The Cotton effects of the
13 adjacent dimer **SQ-BC** at 704 nm ($\Delta\epsilon = +135 \text{ M}^{-1} \text{ cm}^{-1}$), 660 nm ($\Delta\epsilon = -70 \text{ M}^{-1} \text{ cm}^{-1}$) and 640
14 nm ($\Delta\epsilon = -100 \text{ M}^{-1} \text{ cm}^{-1}$) appeared to be less pronounced, possibly due to conformational
15 flexibility. Thus, the CD spectra provide additional confirmation of excitonic delocalization in
16 both squaraine dimers.
17
18

19 As one of the most promising DNA-templated Cy5 aggregates reported by Cannon *et al.*¹⁰⁰⁻¹⁰¹
20 was the tetramer configuration, we proceeded to prepare and characterize the Square 660
21 tetramer aggregates templated by DNA HJs. The electronic absorption spectrum of tetramer **SQ-**
22 **ABCD** exhibited major bands most noticeable at 618 nm and 662 nm (**Fig. 2g**). The most
23 prominent band at 618 nm is further blue-shifted and intensified compared with both adjacent
24 and transverse dimers. Analogous to dimer fitting, a 4-component Gaussian fitting confirmed
25 two strong spectral bands A_2 and A_3 with peak positions of 663 nm and 618 nm, and an
26 additional, weaker band A_1 peaking at 694 nm (**Fig. S7d**). The energy difference A_1-A_2 in **SQ-**
27 **ABCD** was determined to be 84 meV (673 cm⁻¹) and the energy difference A_1-A_3 to be 220 meV
28
29

(1771 cm^{-1}), which, as per above, correspond to large estimated excitonic hopping parameter values of 42 meV (337 cm^{-1}) and 110 meV (886 cm^{-1}), respectively. We also observed continued redistribution of the oscillator strength toward higher-energy absorption bands as seen in the increase of A_2/A_1 and A_3/A_1 intensities. In the CD spectrum, a tetramer **SQ-ABCD** exhibited a strikingly intense exciton-induced negative couplet signal with a couplet amplitude $A = 710 \text{ M}^{-1}$ cm^{-1} (**Fig. 2h**). The symmetry of tetramer CD couplet with similarly intense Cotton effects at 621 nm ($\Delta\epsilon = 310 \text{ M}^{-1} \text{ cm}^{-1}$) and at 688 nm ($\Delta\epsilon = -400 \text{ M}^{-1} \text{ cm}^{-1}$) indicates the presence of a single chiral system composed of strongly coupled Square 660 dyes packing in the form of an H-aggregate. **SQ-ABCD** clearly exhibits signatures of strong excitonic Coulombic coupling.

In addition to strong perturbations to the electronic absorption spectrum and strong CD signals, significant fluorescence quenching was observed in the DNA HJ Square 660 dye dimers and tetramer (**Fig. S5**). Specifically, the relative fluorescence intensity for the different DNA Square 660 dye constructs dropped in the order of **SQ-A** \gg **SQ-AC** $>$ **SQ-BC** $>$ **SQ-ABCD** (**Fig. S5**) with Φ_F values of 0.038, 0.023, and 0.006 measured for **SQ-AC**, **SQ-BC** and **SQ-ABCD**, respectively (**Tbl. 1, Section S5**). The significantly reduced fluorescence intensity indicates that fluorescence emission is strongly quenched in **SQ-AC**, **SQ-BC**, and **SQ-ABCD**. Fluorescence quenching, which is typically due to drastically shortened excited-state lifetimes, has been reported previously in squaraine dimers covalently-bound via methylene bridge linkers.¹²¹ While not a direct indicator of excitonic Coulombic coupling strength, this pioneering report by Liang *et al.* showed that the most strongly-coupled squaraine dimers exhibited the most significant excited state quenching. More recently, similar observations were made in strongly coupled Cy3 and Cy5 aggregates templated in the form of dsDNA and DNA HJs, respectively.^{84, 119}

Theoretical Spectral Modeling

In order to determine the values of the excitonic hopping parameters between dye pairs in each aggregate and obtain quantitative information about the spatial arrangement of the dye molecules in their aggregates, we performed theoretical modeling based on a Kuhn-Renger-May (KRM) model¹²² following the previously described procedure¹⁰⁰⁻¹⁰¹ with some modifications (**Section S9**). This method takes into account the effects of the dominant vibronic mode of each dye in a nonperturbative manner. In brief, the model generates theoretical absorbance and CD spectra of various dye configurations and compares them with experimental absorption and CD spectra (**Fig. 2**). The theoretical dye configuration that yields best-fit spectra to the experimental absorbance and CD spectra is found by a stochastic gradient search. Since the spacing between dyes is typically on the order of or smaller than the dye length, an extended dipole approximation was employed in which the charge distribution is approximated by point charges separated by a distance that is comparable to the dye length.²³ The Hilbert space included all configuration basis states for which the number of quanta of vibration on any dye belongs to the set {0, 1, 2}. Computed eigenvalues and eigenvectors of the Holstein-like Hamiltonian¹²³ showed electronic versus vibronic contribution to energy eigenstates (**Figs. S9 and S10**) confirming the importance of considering vibronic interactions. It is important to note that the KRM model treats an aggregate system as a pure state system. However, it is possible that some structural heterogeneity might be present in squaraine aggregates due to the weak van der Waals forces binding the dyes or DNA structure effects such as conformational isomers of stacked DNA HJ. Consequently, the KRM model results correspond to the dominant average configuration of the dye aggregate. Examination of the alternative transverse dimer **SQ-BD** (**Section S10**) revealed that conformational isomers of DNA HJ are, however, not a primary source of structural

heterogeneity, and that dye-dye interactions play a predominant role in the aggregate packing. The goodness of the fit was evaluated with several parameters: integral overlap between the corresponding absorbance and CD spectra, a mean-square deviation (MSD) and the weighted average of the MSD of the absorbance and CD spectra (**Tbl. S8**). The dye positions were extracted from the fit in terms of the zenith and azimuthal angles, and Cartesian coordinates (**Tbls. S9 and S10**). The dye orientation vectors (**Figs. S11 and S12**) were visualized by means of Avogadro and UCSF Chimera software¹²⁴ (**Fig. 3** and **4**). In order to describe dyes' mutual orientation within an aggregate, such geometric parameters as a center-to-center distance R , a slip angle θ_s and an oblique angle α were extracted from the polar coordinates.

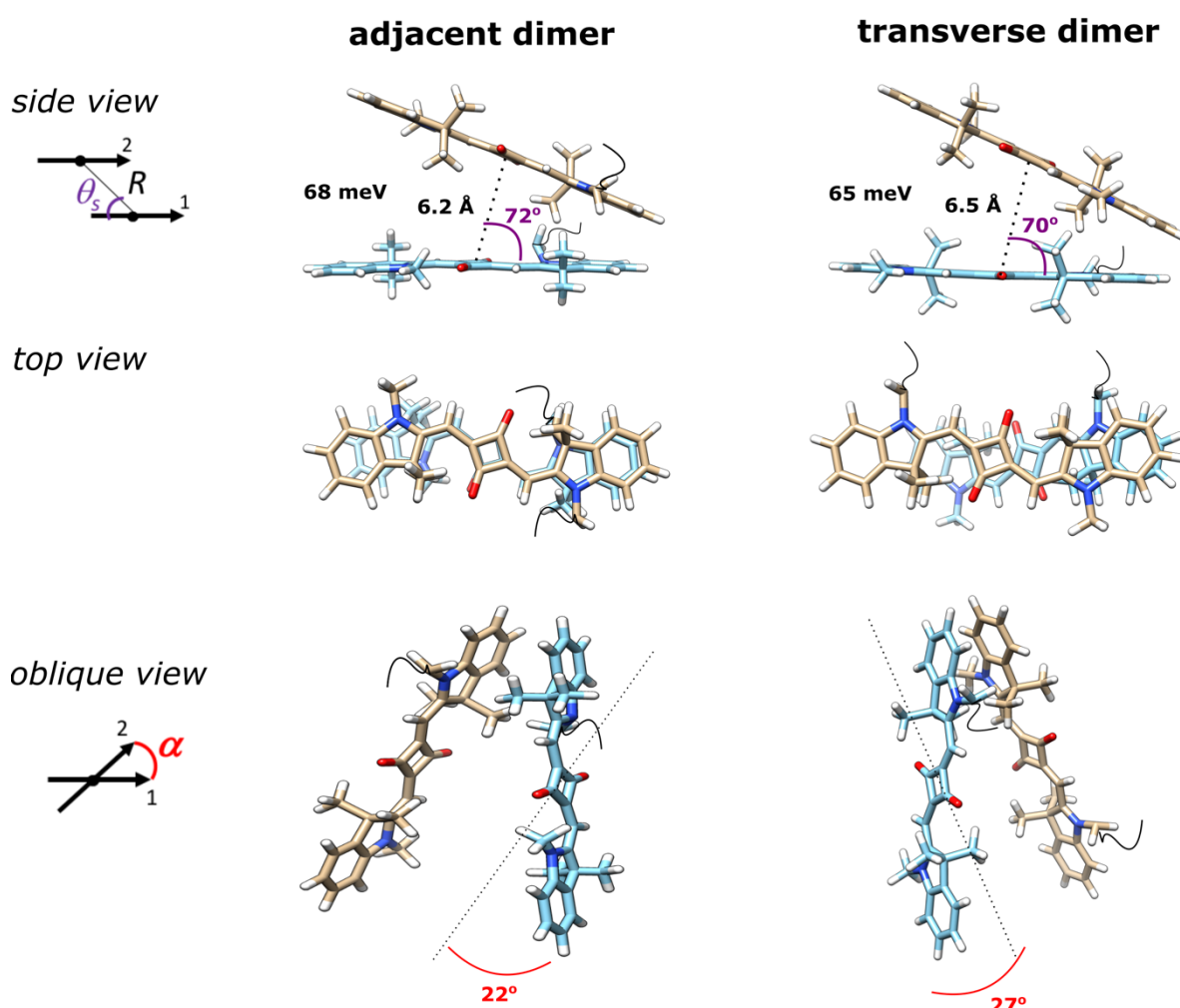


Figure 3. Molecular models of the Square 660 core region adjacent dimer **SQ-BC** and transverse dimer **SQ-AC**. The side view shows a center-to-center distance R in Å and a slip angle θ_s . The top view shows oblique angle α as an angle between vectors 1 and 2 if their centers are superimposed. Note, that the fitting procedure determines the position and orientation of the long axes of the Square 660 dyes, but not the rotation of the dye core around its long axis. As such, the dye core rotations were arbitrary chosen.

In this manner, we first determined a transition dipole moment of monomer **SQ-A** to be 11.7 D by fitting its absorption spectrum thus accounting for the possible electronic interactions between the squaraine dyes and neighboring bases. Next, we calculated the characteristic hopping parameter constant $J_0 = 48 \text{ meV} \cdot \text{nm}^3$ derived from the transition dipole moment of the monomer **SQ-A** following the equation (eq S5). The constant J_0 as a numerical coefficient defines the distances between the molecules extracted by fitting the absorbance and CD spectra in KRM model predictions for dye aggregates. Since J_0 eliminates the degeneracy between the excitonic hopping parameter and spacing between the dyes, more definite predictions for the mutual orientation of the dye molecules are obtained.

Applying the constant J_0 as an input parameter in theoretical fitting of absorption and CD spectra, excitonic hopping parameter values $J_{1,2}$ between dyes in dimer aggregates were obtained (Tbl. S11). The excitonic hopping parameter $J_{1,2}$ between squaraines was found to be 65 meV and 68 meV in the transverse and adjacent dimers respectively. Theoretical fitting of the transverse **SQ-AC** and adjacent **SQ-BC** dimers determined that the dyes are oriented with predominant H-aggregate character exhibiting a slip angle of 70° and 72° respectively (Fig. 3). The center-to-center distance between squaraine molecules in transverse **SQ-AC** and adjacent **SQ-BC** dimers were calculated to be 6.5 Å and 6.2 Å respectively. The transverse dimer exhibited a slightly larger oblique angle α of 27° likely resulting in an experimentally observed more profound CD couplet. Interestingly, the adjacent and transverse dimers show nearly mirror symmetry of their 3-D structures. This observation of a chiral relationship between two dimer configurations is supported by similarity of absorption spectra, and, particularly by circular dichroism showing opposite handedness of analogical spectral line shapes. The optimized modeling procedure was also applied to the H-type Cy5 transverse dimer¹⁰¹ in order to obtain its

*J*_{1,2} value for direct comparison with excitonic Coulombic coupling in squaraine dimers. The excitonic hopping parameter in the H-type Cy5 dimer was determined to be 70 meV. The Cy5 dimer was found to adopt a very similar H-aggregate geometry (**Fig. S13**) compared to the geometry of squaraine dimers **SQ-AC** and **SQ-BC**. The Cy5 molecules in the Cy5 dimer were found to be 5.3 Å apart and characterized by a 76° slip angle and a 18° oblique angle. A slightly higher *J*_{1,2} value in Cy5 dimer is attributed to a shorter center-to-center distance between the Cy5 molecules. These results indicate that squaraines excitonically couple as strong as Cy5 dyes within a comparable dimer configuration.

Theoretical modeling of squaraine tetramer **SQ-ABCD** afforded a matrix of *J*_{m,n} values (**Tbl. S12, Fig. S14**) and revealed geometric details of four molecule positions within the tetramer. Three squaraine molecules were found to form an H-stack with a slight zigzag character while the fourth squaraine positioned out of the H-stack (**Fig. 4**). A mutual arrangement of dyes 1 and 2 closely resembles the adjacent dimer configuration **SQ-BC** as an internal dimer unit within the tetramer. The dyes 1 and 2 in the tetramer are positioned 6.1 Å apart exhibiting an excitonic hopping parameter of 66 meV which value is similar to excitonic hopping in the squaraine dimers. In contrast, while a mutual orientation of dyes 2 and 3 in the tetramer resembles the transverse dimer configuration **SQ-AC**, the excitonic hopping parameter for the dye pair 2-3 is less than in the **SQ-AC**. The center-to-center distance and the oblique angle in the dye pair 2-3 corresponds to the transverse dimer configuration **SQ-AC**, but the slip angle in the dye pair 2-3 is 15° larger than in **SQ-AC** (85° vs 70°). The difference in the slip angle might account for a smaller *J*_{1,2} value observed between dyes 2 and 3 within the tetramer. This observation demonstrates how geometric parameters, in particular, a slip angle affects the excitonic Coulombic coupling between two dyes. Being positioned further from the 3-dye stack (average

18 Å), dye 4 weakly couples with the other three dyes (2.8-6.8 meV). The observed exclusion of dye 4 from the stack is presumably due to steric constraints. The nature of these steric constraints as well as a position of the tetramer relative to the DNA HJ cavity have not yet been identified. For comparison purpose, we determined the values of the excitonic hopping parameters between the dyes in the Cy5 tetramer (Tbl. S13, Fig. S15). While the excitonic hopping strengths between equidistant Square 660 dyes and Cy5 dyes are comparable, the proximity of all four H-stacked Cy5 dyes in a parallelogram-like arrangement¹⁰¹ results in a very intense blue-shifted absorption of the Cy5 tetramer. Perhaps the parallelogram-like arrangement observed in the Cy5 tetramer could also be observed in the Square 660 tetramer if Square 660 dyes were tethered to the DNA with dual phosphoramidite linkers.

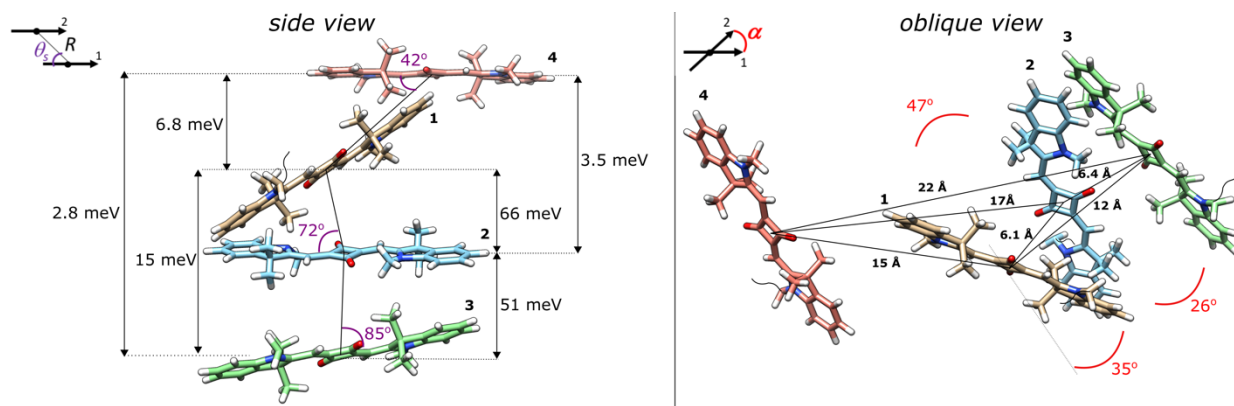


Figure 4. Molecular model of the Square 660 core region tetramer **SQ-ABCD**. The side view $J_{m,n}$ parameter between each pair of dyes in meV and slip angles θ_s °. The oblique view shows a center-to-center distance R in Å and oblique angle α °.

CONCLUSIONS

In this study, we demonstrate that Square 660, a commercially available indolenine squaraine dye, exhibits exciton delocalization when aggregated via a DNA HJ. DNA HJs were used to template the aggregation of Square 660 in three different configurations: a transverse dimer, an adjacent dimer, and a tetramer. Exciton delocalization was evident in all configurations via significant blue shifts in the electronic absorption spectra, intense couplets in the CD spectra, and strong fluorescence emission suppression. Matrices of the excitonic hopping parameter between the dye molecules in dimers and a tetramer were obtained via simultaneous fitting of the absorption and CD spectra. Large values of the excitonic hopping parameters characterized the strength of the exciton Coulombic interactions responsible for exciton delocalization in indolenine squaraine aggregates. The strength of excitonic hopping interactions between indolenine squaraines was found to be comparable with the strength of the analogous DNA HJ templated aggregate of the more ubiquitous cyanine dye Cy5, previously shown to be highly promising for exciton-based applications. An interesting finding of the present work is that DNA HJ templated Square 660 aggregates appear to generally favor an H-type packing configuration regardless of an aggregate configuration, which contrasts with DNA HJ templated aggregates of Cy5 that are capable of adopting both H- and J-type packing arrangements. Based on their superior photostability, structural diversity, and promising aggregate optical properties, we conclude that indolenine squaraine dyes are viable candidates for next-generation technologies where strong excitonic Coulombic coupling and exciton delocalization are desirable, such as artificial light harvesting and potentially even room temperature quantum information systems.

1
2
3 ASSOCIATED CONTENT
4
56 See Supporting Information (PDF) for details pertaining to gel electrophoresis, spectral
7 measurements, thermal denaturation, fitting procedures, and KRM modeling.
8
910
11
12 ACKNOWLEDGMENT
13
1415 This research was supported wholly by the U.S. Department of Energy (DOE), Office of Basic
16 Energy Sciences, Materials Sciences and Engineering Division and DOE's Established Program
17 to Stimulate Competitive Research (EPSCoR) program under Award DE-SC0020089, except as
18 follows: initial work on squaraine transverse dimer modeling was sponsored by National Science
19 Foundation INSPIRE award No. 1648655. The circular dichroism spectrometer was made
20 available through the Biomolecular Research Center (BRC) at Boise State, which is supported in
21 part by the Institutional Development Awards (IDeA) from the National Institute of General
22 Medicine Sciences award No. P20GM103408 and the National Institutes of Health award No.
23 P20GM109095, the National Science Foundation award Nos. 0619793 and 0923535, the MJ
24 Murdock Charitable Trust, and the Idaho State Board of Education. We would like to
25 acknowledge Natalie Magnus and Taylor Farmer and Professor Amit Jain for their assistance in
26 KRM Model Simulation Tool software development.
27
28
29
30
31
32
33
34
35
36
37
38
39
40
41
42
43
44
4546 AUTHOR INFORMATION
47
4849 Corresponding Authors
5051 *(J.L.) E-mail: jeunghoonlee@boisestate.edu
52
5354 *(R.D.P.) E-mail: ryanpensack@boisestate.edu
55
56
57
58
59
60

1
2 *(B.Y.) E-mail: bernardyrurke@boisestate.edu
3
4
5
6 *(W.B.K.) E-mail: bknowlton@boisestate.edu
7
8
9

10 Notes

11

12 E.A.T. is the managing director of SETA BioMedicals, which has an interest in this project.
13
14
15
16

17 REFERENCES

18

- 19 Kasha, M. Energy Transfer Mechanisms and the Molecular Exciton Model for Molecular
20 Aggregates. *Radiat. Res.* **1963**, *20*, 55-70.
- 21 Andrews, D. L. A Unified Theory of Radiative and Radiationless Molecular Energy
22 Transfer. *Chem. Phys.* **1989**, *135*, 195-201.
- 23 Walczak, P. B.; Eisfeld, A.; Briggs, J. S. Exchange Narrowing of the J Band of Molecular
24 Dye Aggregates. *J. Chem. Phys.* **2008**, *128*, 044505.
- 25 Roden, J.; Eisfeld, A. Anomalous Strong Exchange Narrowing in Excitonic Systems. *J.*
26 *Chem. Phys.* **2011**, *134*, 034901.
- 27 Fidder, H.; Knoester, J.; Wiersma, D. A. Optical Properties of Disordered Molecular
28 Aggregates: A Numerical Study. *J. Chem. Phys.* **1991**, *95*, 7880-7890.
- 29 Vaitekonis, S.; Trinkunas, G.; Valkunas, L. Red Chlorophylls in the Exciton Model of
30 Photosystem I. *Photosynth. Res.* **2005**, *86*, 185-201.
- 31 Abramavicius, D.; Mukamel, S. Exciton Delocalization and Transport in Photosystem I
32 of Cyanobacteria Synechococcus Elongates: Simulation Study of Coherent Two-Dimensional
33 Optical Signals. *J. Phys. Chem. B* **2009**, *113*, 6097-6108.
- 34 Abramavicius, D.; Palmieri, B.; Mukamel, S. Extracting Single and Two-Exciton
35 Couplings in Photosynthetic Complexes by Coherent Two-Dimensional Electronic Spectra.
36 *Chem. Phys.* **2009**, *357*, 79-84.
- 37 Abramavicius, D.; Palmieri, B.; Voronine, D. V.; Šanda, F.; Mukamel, S. Coherent
38 Multidimensional Optical Spectroscopy of Excitons in Molecular Aggregates; Quasiparticle
39 Versus Supermolecule Perspectives. *Chem. Rev.* **2009**, *109*, 2350-2408.
- 40 McRae, E. G.; Kasha, M. The Molecular Exciton Model. In *Physical Processes in*
41 *Radiation Biology*, Augenstein, L.; Mason, R.; Rosenberg, B., Eds. Academic Press: New York,
42 1964; pp 23-42.
- 43 Hestand, N. J.; Spano, F. C. Determining the Spatial Coherence of Excitons from the
44 Photoluminescence Spectrum in Charge-Transfer J-Aggregates. *Chem. Phys.* **2016**, *481*, 262-
45 271.
- 46 Hestand, N. J.; Spano, F. C. Molecular Aggregate Photophysics Beyond the Kasha
47 Model: Novel Design Principles for Organic Materials. *Acc. Chem. Res.* **2017**, *50*, 341-350.
- 48 Hestand, N. J.; Spano, F. C. Expanded Theory of H- and J-Molecular Aggregates: The
49 Effects of Vibronic Coupling and Intermolecular Charge Transfer. *Chem. Rev.* **2018**, *118*, 7069-
50 7163.

1
2
3
4
5
6
7
8
9
10
11
12
13
14
15
16
17
18
19
20
21
22
23
24
25
26
27
28
29
30
31
32
33
34
35
36
37
38
39
40
41
42
43
44
45
46
47
48
49
50
51
52
53
54
55
56
57
58
59
50

14. Zhong, C.; Bialas, D.; Collison, C. J.; Spano, F. C. Davydov Splitting in Squaraine
2 Dimers. *Journal of Physical Chemistry C* **2019**, *123*, 18734-18745.
15. Abramavicius, D.; Mukamel, S. Exciton Dynamics in Chromophore Aggregates with
2 Correlated Environment Fluctuations. *J. Chem. Phys.* **2011**, *134*, 174504-174510.
16. Mirkovic, T.; Ostroumov, E. E.; Anna, J. M.; van Grondelle, R.; Govindjee; Scholes, G.
2 D. Light Absorption and Energy Transfer in the Antenna Complexes of Photosynthetic
10 Organisms. *Chem. Rev.* **2017**, *117*, 249-293.
17. Spano, F. C. The Spectral Signatures of Frenkel Polarons in H- and J-Aggregates. *Acc.
2 Chem. Res.* **2010**, *43*, 429-439.
18. Renger, T.; May, V.; Kühn, O. Ultrafast Excitation Energy Transfer Dynamics in
2 Photosynthetic Pigment-Protein Complexes. *Phys. Rep.* **2001**, *343*, 137-254.
19. Schulze, J.; Kühn, O. Explicit Correlated Exciton-Vibrational Dynamics of the FMO
2 Complex. *J. Phys. Chem. B* **2015**, *119*, 6211-6216.
20. Tretiak, S.; Mukamel, S. Density Matrix Analysis and Simulation of Electronic
2 Excitations in Conjugated and Aggregated Molecules. *Chem. Rev.* **2002**, *102*, 3171-3212.
21. Richter, M.; Ahn, K. J.; Knorr, A.; Schliwa, A.; Bimberg, D.; Madjet, M. E.-A.; Renger,
2 T. Theory of Excitation Transfer in Coupled Nanostructures – from Quantum Dots to Light
23 Harvesting Complexes. *Phys. Status Solidi B* **2006**, *243*, 2302-2310.
22. Asanuma, H.; Fujii, T.; Kato, T.; Kashida, H. Coherent Interactions of Dyes Assembled
2 on DNA. *J. Photochem. Photobiol., C* **2012**, *13*, 124-135.
23. Czikkely, V.; Forsterling, H. D.; Kuhn, H. Extended Dipole Model for Aggregates of
2 Dye Molecules. *Chem. Phys. Lett.* **1970**, *6*, 207-210.
24. Jolley, E. E. Spectral Absorption and Fluorescence of Dyes in the Molecular State.
2 *Nature* **1936**, *138*, 1009-1010.
25. Jolley, E. E. Molecular, Nematic and Crystal States of I: I-Diethyl-Cyanine Chloride.
2 *Nature* **1937**, *139*, 631.
26. Scheibe, G. Über Die Veränderlichkeit Der Absorptionsspektren in Lösungen Und Die
2 Nebenvalenzen Als Ihre Ursache. *Angew. Chem.* **1937**, *50*, 212-219.
27. Koepke, J.; Hu, X.; Muenke, C.; Schulten, K.; Michel, H. The Crystal Structure of the
2 Light-Harvesting Complex II (B800-850) from Rhodospirillum Molischianum. *Structure* **1996**,
4, 581-597.
28. Chachisvilis, M.; Kuhn, O.; Pullerits, T.; Sundstrom, V. Excitons in Photosynthetic
2 Purple Bacteria: Wavelike Motion or Incoherent Hopping? *J. Phys. Chem. B* **1997**, *101*, 7275-
41 7283.
29. Hu, X.; Damjanovic, A.; Ritz, T.; Schulten, K. Architecture and Mechanism of the Light-
2 Harvesting Apparatus of Purple Bacteria. *Proc. Natl. Acad. Sci. U. S. A.* **1998**, *95*, 5935-5941.
30. Jonas, D. M.; Lang, M. J.; Nagasawa, Y.; Joo, T.; Fleming, G. R. Pump-Probe
2 Polarization Anisotropy Study of Femtosecond Energy Transfer within the Photosynthetic
47 Reaction Center of Rhodobacter Sphaeroides R26. *J. Phys. Chem.* **1996**, *100*, 12660-12673.
31. Arpin, P. C.; Turner, D. B.; McClure, S. D.; Jumper, C. C.; Mirkovic, T.; Challa, J. R.;
2 Lee, J.; Teng, C. Y.; Green, B. R.; Wilk, K. E., et al. Spectroscopic Studies of Cryptophyte Light
50 Harvesting Proteins: Vibrations and Coherent Oscillations. *J. Phys. Chem. B* **2015**, *119*, 10025-
51 10034.
32. Brixner, T.; Hildner, R.; Kohler, J.; Lambert, C.; Wurthner, F. Exciton Transport in
2 Molecular Aggregates - from Natural Antennas to Synthetic Chromophore Systems. *Adv. Energy
55 Mater.* **2017**, *7*, 1700236.

1
2
3 33. Graugnard, E.; Kellis, D. L.; Bui, H.; Barnes, S.; Kuang, W.; Lee, J.; Hughes, W. L.;
4 Knowlton, W. B.; Yurke, B. DNA-Controlled Excitonic Switches. *Nano Lett.* **2012**, *12*, 2117-
5 2122.
6
7 34. Cannon, B. L.; Kellis, D. L.; Davis, P. H.; Lee, J.; Kuang, W.; Hughes, W. L.;
8 Graugnard, E.; Yurke, B.; Knowlton, W. B. Excitonic and Logic Gates on DNA Brick
9 Nanobreadboards. *ACS Photonics* **2015**, *2*, 398-404.
10
11 35. Kellis, D. L.; Rehn, S. M.; Cannon, B. L.; Davis, P. H.; Graugnard, E.; Lee, J.; Yurke, B.;
12 Knowlton, W. B. DNA-Mediated Excitonic Upconversion FRET Switching. *New J. Phys.* **2015**,
13 *17*, 115007.
14
15 36. Wang, S. Y.; Lebeck, A. R.; Dwyer, C. Nanoscale Resonance Energy Transfer-Based
16 Devices for Probabilistic Computing. *Ieee Micro* **2015**, *35*, 72-84.
17
18 37. Sawaya, N. P. D.; Rappoport, D.; Tabor, D. P.; Aspuru-Guzik, A. Excitonics: A Set of
19 Gates for Molecular Exciton Processing and Signaling. *ACS Nano* **2018**, *12*, 6410-6420.
20
21 38. Ostroverkhova, O. Organic Optoelectronic Materials: Mechanisms and Applications.
22 *Chem. Rev.* **2016**, *116*, 13279-13412.
23
24 39. Bardeen, C. J. The Structure and Dynamics of Molecular Excitons. *Annu. Rev. Phys.*
25 *Chem.* **2014**, *65*, 127-148.
26
27 40. Eisfeld, A.; Briggs, J. S. The J-Band of Organic Dyes: Lineshape and Coherence Length.
28 *Chem. Phys.* **2002**, *281*, 61-70.
29
30 41. Thilagam, A. Entanglement Dynamics of J-Aggregate Systems. *J. Phys. A: Math. Theor.*
31 **2011**, *44*, 135306.
32
33 42. Sarovar, M.; Ishizaki, A.; Fleming, G. R.; Whaley, K. B. Quantum Entanglement in
34 Photosynthetic Light-Harvesting Complexes. *Nat. Phys.* **2010**, *6*, 462-467.
35
36 43. Thilagam, A. *Quantum Information Processing Attributes of J-Aggregates*. World
37 Scientific Publishing Company: Singapore, 2012; Vol. 2.
38
39 44. Ball, P. Physics of Life: The Dawn of Quantum Biology. *Nature* **2011**, *474*, 272-274.
40
41 45. Lloyd, S. Quantum Coherence in Biological Systems. *J. Phys.: Conf. Ser.* **2011**, *302*,
42 012037.
43
44 46. Vickerstaff, T.; Lemm, D. R. Aggregation of Dyes in Aqueous Solution. *Nature* **1946**,
45 *157*, 373-373.
46
47 47. Dickinson, H. O. The Aggregation of Cyanine Dyes in Aqueous Solution. *Trans. Faraday Soc.* **1947**, *43*, 486-491.
48
49 48. Heyne, B. Self-Assembly of Organic Dyes in Supramolecular Aggregates. *Photochem. Photobiol. Sci.* **2016**, *15*, 1103-1114.
50
51 49. Engel, G. S.; Calhoun, T. R.; Read, E. L.; Ahn, T. K.; Mancal, T.; Cheng, Y. C.;
52 Blankenship, R. E.; Fleming, G. R. Evidence for Wavelike Energy Transfer through Quantum
53 Coherence in Photosynthetic Systems. *Nature* **2007**, *446*, 782-786.
54
55 50. Lee, H.; Cheng, Y. C.; Fleming, G. R. Coherence Dynamics in Photosynthesis: Protein
56 Protection of Excitonic Coherence. *Science* **2007**, *316*, 1462-1465.
57
58 51. Scholes, G. D.; Fleming, G. R.; Olaya-Castro, A.; van Grondelle, R. Lessons from Nature
59 About Solar Light Harvesting. *Nat. Chem.* **2011**, *3*, 763-774.
60
61 52. Scholes, G. D. Quantum Biology Coherence in Photosynthesis. *Nat. Phys.* **2011**, *7*, 448-
62 449.
63
64 53. Fassioli, F.; Dinshaw, R.; Arpin, P. C.; Scholes, G. D. Photosynthetic Light Harvesting:
65 Excitons and Coherence. *J. R. Soc., Interface* **2014**, *11*, 20130901.

1
2
3 54. Dill, K. A.; MacCallum, J. L. The Protein-Folding Problem, 50 Years On. *Science* **2012**,
4 338, 1042-1046.
5 55. Yeates, T. O. Geometric Principles for Designing Highly Symmetric Self-Assembling
6 Protein Nanomaterials. *Annu. Rev. Biophys.* **2017**, 46, 23-42.
7 56. Huang, P. S.; Boyken, S. E.; Baker, D. The Coming of Age of De Novo Protein Design.
8 *Nature* **2016**, 537, 320-327.
9 57. Bale, J. B.; Gonen, S.; Liu, Y.; Sheffler, W.; Ellis, D.; Thomas, C.; Cascio, D.; Yeates, T.
10 O.; Gonen, T.; King, N. P., et al. Accurate Design of Megadalton-Scale Two-Component
11 Icosahedral Protein Complexes. *Science* **2016**, 353, 389-394.
12 58. Wei, B.; Dai, M.; Yin, P. Complex Shapes Self-Assembled from Single-Stranded DNA
13 Tiles. *Nature* **2012**, 485, 623-626.
14 59. Ke, Y.; Ong, L. L.; Shih, W. M.; Yin, P. Three-Dimensional Structures Self-Assembled
15 from DNA Bricks. *Science* **2012**, 338, 1177-1183.
16 60. Rothemund, P. W. K. Folding DNA to Create Nanoscale Shapes and Patterns. *Nature*
17 **2006**, 440, 297-302.
18 61. Seeman, N. C. DNA in a Material World. *Nature* **2003**, 421, 427-431.
19 62. Seifert, J. L.; Connor, R. E.; Kushon, S. A.; Wang, M.; Armitage, B. A. Spontaneous
20 Assembly of Helical Cyanine Dye Aggregates on DNA Nanotemplates. *J. Am. Chem. Soc.* **1999**,
21 121, 2987-2995.
22 63. Smith, J. O.; Olson, D. A.; Armitage, B. A. Molecular Recognition of PNA-Containing
23 Hybrids: Spontaneous Assembly of Helical Cyanine Dye Aggregates on PNA Templates. *J. Am.*
24 *Chem. Soc.* **1999**, 121, 2686-2695.
25 64. Wang, M. M.; Silva, G. L.; Armitage, B. A. DNA-Templated Formation of a Helical
26 Cyanine Dye J-Aggregate. *J. Am. Chem. Soc.* **2000**, 122, 9977-9986.
27 65. Chowdhury, A.; Wachsmann-Hogiu, S.; Bangal, P. R.; Raheem, I.; Peteanu, L. A. Characterization of Chiral H and J Aggregates of Cyanine Dyes Formed by DNA Templating
28 Using Stark and Fluorescence Spectroscopies. *J. Phys. Chem. B* **2001**, 105, 12196-12201.
29 66. Garoff, R. A.; Litzinger, E. A.; Connor, R. E.; Fishman, I.; Armitage, B. A. Helical
30 Aggregation of Cyanine Dyes on DNA Templates: Effect of Dye Structure on Formation of
31 Homo- and Heteroaggregates. *Langmuir* **2002**, 18, 6330-6337.
32 67. Chowdhury, A.; Yu, L. P.; Raheem, I.; Peteanu, L.; Liu, L. A.; Yaron, D. J. Stark
33 Spectroscopy of Size-Selected Helical H-Aggregates of a Cyanine Dye Templatized by Duplex
34 DNA. Effect of Exciton Coupling on Electronic Polarizabilities. *J. Phys. Chem. A* **2003**, 107,
35 3351-3362.
36 68. Hannah, K. C.; Armitage, B. A. DNA-Templated Assembly of Helical Cyanine Dye
37 Aggregates: A Supramolecular Chain Polymerization. *Acc. Chem. Res.* **2004**, 37, 845-853.
38 69. Tomlinson, A.; Frezza, B.; Kofke, M.; Wang, M. M.; Armitage, B. A.; Yaron, D. A. Structural Model for Cyanine Dyes Templatized into the Minor Groove of DNA. *Chem. Phys.*
39 **2006**, 325, 36-47.
40 70. Stadler, A. L.; Renikuntla, B. R.; Yaron, D.; Fang, A. S.; Armitage, B. A. Substituent
41 Effects on the Assembly of Helical Cyanine Dye Aggregates in the Minor Groove of a DNA
42 Template. *Langmuir* **2011**, 27, 1472-1479.
43 71. Banal, J. L.; Kondo, T.; Veneziano, R.; Bathe, M.; Schlau-Cohen, G. S. Photophysics of
44 J-Aggregate-Mediated Energy Transfer on DNA. *J. Phys. Chem. Lett.* **2017**, 8, 5827-5833.
45
46
47
48
49
50
51
52
53
54
55
56
57
58
59
60

1
2
3 72. Boulais, E.; Sawaya, N. P. D.; Veneziano, R.; Andreoni, A.; Banal, J. L.; Kondo, T.;
4 Mandal, S.; Lin, S.; Schlau-Cohen, G. S.; Woodbury, N. W., et al. Programmed Coherent
5 Coupling in a Synthetic DNA-Based Excitonic Circuit. *Nat. Mater.* **2018**, *17*, 159-166.
6
7 73. Nicoli, F.; Roos, M. K.; Hemmig, E. A.; Di Antonio, M.; de Vivie-Riedle, R.; Liedl, T.
8 Proximity-Induced H-Aggregation of Cyanine Dyes on DNA-Duplexes. *J. Phys. Chem. A* **2016**,
9 *120*, 9941-9947.
10
11 74. Markova, L. I.; Malinovskii, V. L.; Patsenker, L. D.; Haner, R. J- Vs. H-Type Assembly:
12 Pentamethine Cyanine (Cy5) as a near-IR Chiroptical Reporter. *Chem. Commun.* **2013**, *49*, 5298-
13 5300.
14
15 75. Probst, M.; Langenegger, S. M.; Haner, R. A Modular Lhc Built on the DNA Three-Way
16 Junction. *Chem. Commun.* **2014**, *50*, 159-161.
17
18 76. Markova, L. I.; Malinovskii, V. L.; Patsenker, L. D.; Haner, R. Synthesis and Properties
19 of Squaraine-Modified DNA. *Org. Biomol. Chem.* **2012**, *10*, 8944-8947.
20
21 77. Malinovskii, V. L.; Wenger, D.; Haner, R. Nucleic Acid-Guided Assembly of Aromatic
22 Chromophores. *Chem. Soc. Rev.* **2010**, *39*, 410-422.
23
24 78. Li, S.; Langenegger, S. M.; Haner, R. Control of Aggregation-Induced Emission by DNA
25 Hybridization. *Chem. Commun.* **2013**, *49*, 5835-5837.
26
27 79. Haner, R.; Samain, F.; Malinovskii, V. L. DNA-Assisted Self-Assembly of Pyrene
28 Foldamers. *Chemistry* **2009**, *15*, 5701-5708.
29
30 80. Garo, F.; Haner, R. A DNA-Based Light-Harvesting Antenna. *Angew. Chem., Int. Ed.*
31 *Engl.* **2012**, *51*, 916-919.
32
33 81. Adeyemi, O. O.; Malinovskii, V. L.; Biner, S. M.; Calzaferri, G.; Haner, R. Photon
34 Harvesting by Excimer-Forming Multichromophores. *Chem. Commun.* **2012**, *48*, 9589-9591.
35
36 82. Asanuma, H.; Fujii, T.; Kato, T.; Kashida, H. Coherent Interactions of Dyes Assembled
37 on DNA. *J. Photochem. Photobiol., C* **2012**, *13*, 124-135.
38
39 83. Kashida, H.; Asanuma, H. Preparation of Supramolecular Chromophoric Assemblies
40 Using a DNA Duplex. *Phys. Chem. Chem. Phys.* **2012**, *14*, 7196-7204.
41
42 84. Cunningham, P. D.; Kim, Y. C.; Diaz, S. A.; Buckhout-White, S.; Mathur, D.; Medintz, I.
43 L.; Melinger, J. S. Optical Properties of Vibronically Coupled Cy3 Dimers on DNA Scaffolds. *J.*
44 *Phys. Chem. B* **2018**, *122*, 5020-5029.
45
46 85. Mazuski, R. J.; Diaz, S. A.; Wood, R. E.; Lloyd, L. T.; Klein, W. P.; Mathur, D.;
47 Melinger, J. S.; Engel, G. S.; Medintz, I. L. Ultrafast Excitation Transfer in Cy5 DNA Photonic
48 Wires Displays Dye Conjugation and Excitation Energy Dependency. *J. Phys. Chem. Lett.* **2020**,
49 4163-4172.
50
51 86. Asanuma, H.; Shirasuka, K.; Takarada, T.; Kashida, H.; Komiyama, M. DNA-Dye
52 Conjugates for Controllable H Aggregation(1). *J. Am. Chem. Soc.* **2003**, *125*, 2217-2223.
53
54 87. Kashida, H.; Asanuma, H.; Komiyama, M. Alternating Hetero H Aggregation of
55 Different Dyes by Interstrand Stacking from Two DNA-Dye Conjugates. *Angew. Chem., Int. Ed.*
56 *Engl.* **2004**, *43*, 6522-6525.
57
58 88. Kashida, H.; Tanaka, M.; Baba, S.; Sakamoto, T.; Kawai, G.; Asanuma, H.; Komiyama, M.
59 Covalent Incorporation of Methyl Red Dyes into Double-Stranded DNA for Their Ordered
60 Clustering. *Chem. - Eur. J.* **2006**, *12*, 777-784.
61
62 89. Ikeda, S.; Okamoto, A. Hybridization-Sensitive On-Off DNA Probe: Application of the
63 Exciton Coupling Effect to Effective Fluorescence Quenching. *Chem. - Asian J.* **2008**, *3*, 958-
64 968.

1
2
3 90. Fujii, T.; Kashida, H.; Asanuma, H. Analysis of Coherent Heteroclustering of Different
4 Dyes by Use of Threoninol Nucleotides for Comparison with the Molecular Exciton Theory.
5 *Chem. - Eur. J.* **2009**, *15*, 10092-10102.

6 91. Hara, Y.; Fujii, T.; Kashida, H.; Sekiguchi, K.; Liang, X.; Niwa, K.; Takase, T.; Yoshida,
7 Y.; Asanuma, H. Coherent Quenching of a Fluorophore for the Design of a Highly Sensitive in-
8 Stem Molecular Beacon. *Angew. Chem., Int. Ed. Engl.* **2010**, *49*, 5502-5506.

9 92. Ruedas-Rama, M. J.; Alvarez-Pez, J. M.; Orte, A. Formation of Stable BOBO-3 H-
10 Aggregate Complexes Hinders DNA Hybridization. *J. Phys. Chem. B* **2010**, *114*, 9063-9071.

11 93. Ruedas-Rama, M. J.; Orte, A.; Martin-Domingo, M. C.; Castello, F.; Talavera, E. M.;
12 Alvarez-Pez, J. M. Interaction of YOYO-3 with Different DNA Templates to Form H-
13 Aggregates. *J. Phys. Chem. B* **2014**, *118*, 6098-6106.

14 94. Kringle, L.; Sawaya, N. P. D.; Widom, J.; Adams, C.; Raymer, M. G.; Aspuru-Guzik, A.;
15 Marcus, A. H. Temperature-Dependent Conformations of Exciton-Coupled Cy3 Dimers in
16 Double-Stranded DNA. *J. Chem. Phys.* **2018**, *148*, 085101.

17 95. Heussman, D.; Kittell, J.; Kringle, L.; Tamimi, A.; von Hippel, P. H.; Marcus, A. H.
18 Measuring Local Conformations and Conformational Disorder of (Cy3)(2) Dimer Labeled DNA
19 Fork Junctions Using Absorbance, Circular Dichroism and Two-Dimensional Fluorescence
20 Spectroscopy. *Faraday Discuss.* **2019**, *216*, 211-235.

21 96. Albinsson, B.; Hannestad, J. K.; Börjesson, K. Functionalized DNA Nanostructures for
22 Light Harvesting and Charge Separation. *Coord. Chem. Rev.* **2012**, *256*, 2399-2413.

23 97. Probst, M.; Wenger, D.; Biner, S. M.; Haner, R. The DNA Three-Way Junction as a
24 Mould for Tripartite Chromophore Assembly. *Org. Biomol. Chem.* **2012**, *10*, 755-759.

25 98. Seeman, N. C. Nucleic Acid Junctions and Lattices. *J. Theor. Biol.* **1982**, *99*, 237-247.

26 99. Kallenbach, N. R.; Ma, R.-I.; Seeman, N. C. An Immobile Nucleic Acid Junction
27 Constructed from Oligonucleotides. *Nature* **1983**, *305*, 829-831.

28 100. Cannon, B. L.; Kellis, D. L.; Patten, L. K.; Davis, P. H.; Lee, J.; Graugnard, E.; Yurke,
29 B.; Knowlton, W. B. Coherent Exciton Delocalization in a Two-State DNA-Templated Dye
30 Aggregate System. *J. Phys. Chem. A* **2017**, *121*, 6905-6916.

31 101. Cannon, B. L.; Patten, L. K.; Kellis, D. L.; Davis, P. H.; Lee, J.; Graugnard, E.; Yurke,
32 B.; Knowlton, W. B. Large Davydov Splitting and Strong Fluorescence Suppression: An
33 Investigation of Exciton Delocalization in DNA-Templated Holliday Junction Dye Aggregates.
34 *J. Phys. Chem. A* **2018**, *122*, 2086-2095.

35 102. Davydov, A. Theory of Absorption Spectra of Molecular Crystals. *Ukr. J. Phys.* **2008**,
36 *53*, 69-70.

37 103. Stennett, E. M. S.; Ciuba, M. A.; Levitus, M. Photophysical Processes in Single Molecule
38 Organic Fluorescent Probes. *Chem. Soc. Rev.* **2014**, *43*, 1057-1075.

39 104. Demchenko, A., P. Photobleaching of Organic Fluorophores: Quantitative
40 Characterization, Mechanisms, Protection. *Methods Appl. Fluoresc.* **2020**, *8*, 022001.

41 105. Yagi, S.; Nakazumi, H. In *Heterocyclic Polymethine Dyes. Topics in Heterocyclic*
42 *Chemistry*, Strekowski, L., Ed. Springer-Verlag: Berlin, Heidelberg, 2008; Vol. 14, pp 133-181.

43 106. Terpetschnig, E.; Szmacinski, H.; Lakowicz, J. R. Synthesis, Spectral Properties and
44 Photostabilities of Symmetrical and Unsymmetrical Squaraines - a New Class of Fluorophores
45 with Long-Wavelength Excitation and Emission. *Anal. Chim. Acta* **1993**, *282*, 633-641.

46 107. Terpetschnig, E.; Lakowicz, J. R. Synthesis and Characterization of Unsymmetrical
47 Squaraines - a New Class of Cyanine Dyes. *Dyes Pigm.* **1993**, *21*, 227-234.

1
2
3 108. Markova, L. I.; Terpetschnig, E. A.; Patsenker, L. D. Comparison of a Series of
4 Hydrophilic Squaraine and Cyanine Dyes for Use as Biological Labels. *Dyes Pigm.* **2013**, *99*,
5 561-570.

6 109. Treibs, Z. J., K. . Cyclotrimethine Dyes Derived from Squaric Acid. *Angew. Chem. Int.*
7 *Ed.* **1965**, *4*, 694.

8 110. Jiang, J. Q.; Sun, C. L.; Shi, Z. F.; Zhang, H. L. Squaraines as Light-Capturing Materials
9 in Photovoltaic Cells. *RSC Adv.* **2014**, *4*, 32987-32996.

10 111. Khopkar, S.; Shankarling, G. Synthesis, Photophysical Properties and Applications of
11 NIR Absorbing Unsymmetrical Squaraines: A Review. *Dyes Pigm.* **2019**, *170*, 107645.

12 112. Sivaramapanner, S. P., C.; Parayalil, C. Ayyappanpillai A. Squaraine Dyes: A Mine of
13 Molecular Materials. *J. Mater. Chem.* **2008**, *18*, 264-274.

14 113. Xia, G. M.; Wang, H. M. Squaraine Dyes: The Hierarchical Synthesis and Its Application
15 in Optical Detection. *J. Photochem. Photobiol., C* **2017**, *31*, 84-113.

16 114. Ilina, K.; MacCuaig, W. M.; Laramie, M.; Jeouty, J. N.; McNally, L. R.; Henary, M.
17 Squaraine Dyes: Molecular Design for Different Applications and Remaining Challenges.
18 *Bioconjugate Chem.* **2020**, *31*, 194-213.

19 115. Wurthner, F.; Kaiser, T. E.; Saha-Moller, C. R. J-Aggregates: From Serendipitous
20 Discovery to Supramolecular Engineering of Functional Dye Materials. *Angew. Chem., Int. Ed.*
21 *Engl.* **2011**, *50*, 3376-3410.

22 116. Mayerhoffer, U.; Wurthner, F. Cooperative Self-Assembly of Squaraine Dyes. *Chem. Sci.*
23 **2012**, *3*, 1215-1220.

24 117. Röhr, M. I. S.; Marciniak, H.; Hoche, J.; Schreck, M. H.; Ceymann, H.; Mitric, R.;
25 Lambert, C. Exciton Dynamics from Strong to Weak Coupling Limit Illustrated on a Series of
26 Squaraine Dimers. *J. Phys. Chem. C* **2018**, *122*, 8082-8093.

27 118. Malý, P.; Lüttig, J.; Mueller, S.; Schreck, M.; Lambert, C.; Brixner, T. Coherently and
28 Fluorescence-Detected Two-Dimensional Electronic Spectroscopy: Direct Comparison on
29 Squaraine Dimers. *Phys. Chem. Chem. Phys.* **2020**, DOI: 10.1039/d1030cp03218b.

30 119. Huff, J. S.; Davis, P. H.; Christy, A.; Kellis, D. L.; Kandadai, N.; Toa, Z. S. D.; Scholes,
31 G. D.; Yurke, B.; Knowlton, W. B.; Pensack, R. D. DNA-Templated Aggregates of Strongly
32 Coupled Cyanine Dyes: Nonradiative Decay Governs Exciton Lifetimes. *J. Phys. Chem. Lett.*
33 **2019**, *10*, 2386-2392.

34 120. Spano, F. C. Analysis of the Uv/Vis and Cd Spectral Line Shapes of Carotenoid
35 Assemblies: Spectral Signatures of Chiral H-Aggregates. *J. Am. Chem. Soc.* **2009**, *131*, 4267-
36 4278.

37 121. Liang, K. N.; Farahat, M. S.; Perlstein, J.; Law, K. Y.; Whitten, D. G. Exciton
38 Interactions in Nonconjugated Squaraine Dimers. Mechanisms for Coupling and Consequences
39 for Photophysics and Photochemistry. *J. Am. Chem. Soc.* **1997**, *119*, 830-831.

40 122. Kuhn, O.; Renger, T.; May, V. Theory of Exciton-Vibrational Dynamics in Molecular
41 Dimers. *Chem. Phys.* **1996**, *204*, 99-114.

42 123. Holstein, T. Studies of Polaron Motion: Part I. The Molecular-Crystal Model. *Ann. Phys.*
43 **1959**, *8*, 325-342.

44 124. Pettersen, E. F.; Goddard, T. D.; Huang, C. C.; Couch, G. S.; Greenblatt, D. M.; Meng, E.
45 C.; Ferrin, T. E. Ucsf Chimera - a Visualization System for Exploratory Research and Analysis.
46 *J. Comput. Chem.* **2004**, *25*, 1605-1612.

TOC Graphic

